Digital image-based analysis of a small-scale dam failure during wetting

Gerardo Morales[1,2], *Núria M.* Pinyol[1,2], and *Antonio* Lloret[1]

[1]Centre de Metodes Numerics en Enginyeria (CIMNE), Barcelona, Spain
[2]Department of Civil and Environmental Engineering, Universitat Politècnica de Catalunya (UPC), Barcelona, Spain

Abstract. The use of digital images and the correlation of them in time is commonly used in geotechnical laboratory experiments to measure surface variables in a non-invasive and massive way. Digital image correlation-based methods provide a measure of the motion of soil. More recently, measurements of the degree of saturation on soil surface using digital images have also been developed, although its application and validation are still limited. This methodology is based on the fact that almost all soils become darker (less light reflective) due to wetting. This article uses image-based analysis techniques to evaluate the behaviour during wetting of a small-scale dam made of compacted fine sand. With the aim of validating the measurements from images, soil moisture sensors were installed in the dam. The tested soil was previously calibrated to determine the correlation of light reflectance and the degree of saturation covering from dry to fully saturated range. Measurements of velocity, displacements, deformations and the degree of saturation in time are evaluated during the experiment based on images recorded in the visual and shortwave infrared (SWIR) light range. The methodology is described step-by-step including camera and lighting system, sample preparation, image acquisition and image analysis. The techniques used allow the changes in the degree of saturation in soil in motion and the failure mechanisms associated with the wetting process to be observed. The results obtained through image analyses show good agreement with the parameters obtained in point measurements with conventional sensors. The results also show some limitations of the method, mainly associated with the accumulation of errors in the tracking of soil particles during large displacements.

1 Introduction

Geotechnical physical models are often used to complement and validate numerical and analytical models because they provide a more realistic approach to the field behaviour of geological media. Physical models can be done at large, medium or small scale, the selection of the scale will be the result of considering different factors such as the problem under study, experimental reproducibility, available measurement techniques, and the economic cost involved in the development of the experiment. If the problem under study involves the control of the boundary conditions and high reproducibility, a small-scale model may be the most suitable option and the measurement of variables will be crucial to the analysis of the model behaviour.

In laboratory experiments of unsaturated porous media, the measurement of water related variables such as pore-water pressure, degree of saturation, moisture content, and suction are often carried out through the installation of sensors such as PPTs, TDR moisture sensors and tensiometers. Although the use of these sensors is highly reliable, when dealing with small scale physical models two limitations need to be addressed. First, these sensors measure data at discrete localised volumes of the soil sample, which could be difficult to interpret and show 2D results. Of course, this limitation could be overcome by installing more sensors, but a highly instrumented model could lead to the second limitation: conventional sensors with intrusive nature could alter the mechanical behaviour of the model. This invasive effect becomes more evident when studying large-strain problems [1] such as landslides and earth dam failures. Alternatively, digital image correlation techniques offer a non-invasive way to measure surface data at high spatio-temporal resolution.

In this regard, particle image velocimetry (PIV) [2] is used to measure displacement, velocity and acceleration using consecutive digital images. The calculations are performed at the centre of fixed subsets of the image. This technique has grown in popularity among the geotechnical research community over the past decade because of the technologic upgrade of digital cameras and the availability of open-source software such as PIVlab, GeoPIV and GeoPIV-RG [3-5]. Further, for large-strain problems the PIV-NP technique [6] also measures the cumulative displacement and trajectory of numerical particles. However, it is important to point out that experimental key aspects such as camera calibration, soil texture and illumination could lead to calculation errors of displacement and velocity [7].

Digital images can also be used to measure the surface degree of saturation of soil in images taken at the visual range [8-10] or at the short-wave infrared (SWIR) range [11-17] of the electromagnetic spectrum. This image correlation methodologies are based on the

principle that almost all soils become darker (less light reflective) during wetting.

This paper presents the evaluation of a small-scale laboratory experiment at 1g. The model under study corresponds to an earth dam, the failure is triggered due to water table rise at the upstream slope. Images in the visual range were used to analyse deformations and displacements with the PIV-NP technique, while the measurements of the surface degree of saturation were carried out through images in the infrared SWIR range of the electromagnetic spectrum. Additionally, capacitance moisture sensors were placed at fixed positions within the model to validate the results obtained from the infrared images.

2 Basic concepts of image analysis

2.1 PIV and PIV-NP

The Particle Image Velocimetry (PIV) proposed by Adrian [2] for fluid mechanics has been successfully applied in geotechnical engineering laboratory experiments through open-source codes such as PIVlab, GeoPIV and GeoPIV-RG [3-5]. The PIV technique calculates the pixel displacement between subsequent images. To do so, it discretizes a reference image into subsets and uses cross-correlation algorithms to locate each subset in a target image. Then, the measured displacement at image space (pixels) is calibrated into object space (length) based on control points previously placed on the experiment at known fixed coordinates. Further, by imposing the time step between the consecutive images, PIV calculates the velocity and acceleration of each subset and other derivatives such as deformations and strain rates. In PIV each measurement is performed at fixed positions which are the centre of each subset.

Suitable for large-strain problems, Pinyol & Alvarado [6] proposed the PIV-NP technique. The PIV-NP consists in post-processing the PIV results calculated at fixed points through a Eulerian approach. The displacement measurements at fixed points in the space are stored on nodes of a predefined support mesh and mapped, by means of linear shape functions, to numerical particles (NP) that represent portions of the moving mass evaluated. It results in a Eulerian-Lagrangian approach in which the reference will not be the fixed centre of subsets where the displacement measures are provided from PIV, but the moving numerical particles itselfs, which is convenient when analysing large deformations.

To successfully perform measurement of displacement and velocity through image analysis, besides the selection of the methodology (PIV or PIV-NP), it is crucial to consider other aspects such as: the selection of the camera and its calibration due to lens distortion; evaluation of the soil texture by exploring the quality of the image; addition of adequate and enough control points; and provide illumination over the exposed plane [7].

2.2 Degree of saturation measured through image analysis

Considering that soils become darker when wetted, digital image processing on the visual range (380 nm – 700 nm) and the short-wave infrared range (1400 nm – 3000 nm) of the electromagnetic spectrum have been proven useful to measure volumetric water content and the degree of saturation in laboratory experiments [1, 8-17].

In digital images, the colour of each pixel, which range from 0 – 255, being 0 totally black and 255 totally white, can be expressed either by RGB (red, green and blue), HSV (hue, saturation and value) or HSB (hue, saturation and brightness) colour system. The methodology employed by Persson [8] applied the RGB and HSV colour system to measure the volumetric water content of four soils with different grain-size distributions. Yoshimoto *et al.* [9], on the other hand, used red food-dye to prepare soil samples at different degrees of saturation (*Sr*), and the digital images of the samples were taken and analysed with the RGB colour system to correlate the degree of saturation to the pixel colour. Later on, Belfort *et al.* [10] evaluated the volumetric water content correlating it with the RGB colour system without using any dye. They proposed a methodology that includes the processing of the images by applying a median filter if necessary, and the normalisation of pixel intensity values. The previously mentioned works and proposed methodologies share some similarities:

- Preparation of soil samples at different moisture conditions.
- Application of constant and even illumination over the exposed plane.
- Digital images on visual range are taken from the soil samples prepared at different moisture conditions.
- Selection of the pixel colour system (RGB, HSV, HSB).
- Individual pixel intensities are not considered, instead, an average intensity value is calculated over a selected sample surface area.
- If necessary, application of median filters and normalization may be done to correct possible fluctuations in light condition.
- The calculated pixel intensity is correlated to the volumetric water content or the degree of saturation of each soil sample.
- Finally, a best fit equation is selected to present an empirical calibration curve to correlate the pixel intensity and the surface soil moisture.

Based again on the principle that soils become darker due to wetting, and considering that soil surface reflectance decreases depending on light wavelength and water content [11-17], full spectroscopy (350 nm – 2500 nm) experiments were developed to study the moisture effect on soil surface reflectance. Lobell & Asner [12], Knadel *et al.* [13], Nolet *et al.* [14], Sadeghi *et al.* [15], and Tian & Philpot [16] noted that reflectance is more sensitive to moisture variations in the NIR and SWIR wavelengths. Light absorption peaks can be

determined between 1400 – 1550 nm and 1900 - 2000 nm [17] (Figure 1).

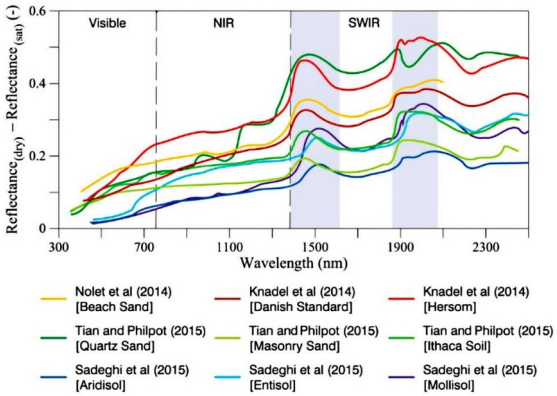

Fig. 1. Difference between dry and saturated surface reflectance for different soils [17]

More recently, Parera *et al.* [17] proposed a methodology to continuously measure the variation of the degree of saturation through infrared images on the SWIR range. The methodology, referred to in this paper as SWIR-Sr technique, proposes the construction of a normalised calibration curve that correlates the surface degree of saturation of soil samples with its reflectance, quantified as pixel intensity or gray value of the infrared images. To do so, soil samples are prepared at different degrees of saturation, infrared light is applied to the soil samples, and images are taken through an infrared camera. To get the gray value of each sample, a Gauss filter is first applied to eliminate the effects of scattering and salt-pepper noise. After that, the pixel intensity representing each sample is correlated to its degree of saturation. Considering that the gray value of pixels depends on the intensity of incident light and in order to determine a calibration curve for a given soil, a normalisation is applied (Equation 1) and a curve correlating the degree of saturation vs normalized gray value curve (Sr vs GVn) is obtained.

$$GV_n = \frac{GV - GV_{sat}}{GV_{dry} - GV_{sat}} \quad (1)$$

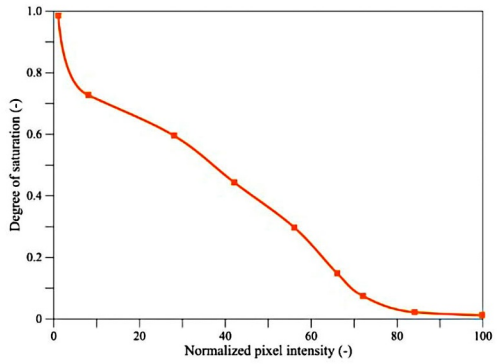

Fig. 2. Calibration curve of correlation between normalized gray value and degree of saturation for Castelldefels beach sand. [17]

The obtained curve can be applied to other laboratory experiments with variations in the lighting conditions as long as the light source emits on the infrared range. Figure 2 shows the calibration curve of a fine beach sand from Castelldefels beach in Catalonia Spain used in the experiments evaluated in this work. A non-linear correlation between pixel intensity and degree of saturation was found for this material.

3 Evaluation of a 1g small-scale dam

3.1 Methodology

This article uses image-based analysis techniques to evaluate the behaviour during wetting of a small-scale dam. The methodology is described step-by-step including: model description, cameras and lighting setup, sample preparation, and image analysis.

Model description:

The case presented in this article consists in the evaluation of the wetting process of a small-scale dam made with the fine beach sand. Figure 3 shows a schematic illustration of the model. The experiment was carried out in a transparent tank (1000 mm length, 400 mm height and 200 mm width). The front wall (transparent window) of the tank is made of glass, meanwhile the other walls of the tank are made of methacrylate. Eight control points were placed over the transparent window at known fixed coordinates that are used as references during image analysis. The model of the dam has 300 mm height, base width of 540 mm and the crown width of 100 mm, its upstream slope is 45º while the downstream slope has a steeper slope with 65º. A wetting process was carried out by lateral water inlet whose flow velocity was imposed to get a water table rise at a rate of 17 mm/min. Six soil moisture sensors were installed, three SKU:SEN0193 sensors from DFRobot and three EC-5 sensors from Meter. The sensors were placed within the model at fixed positions.

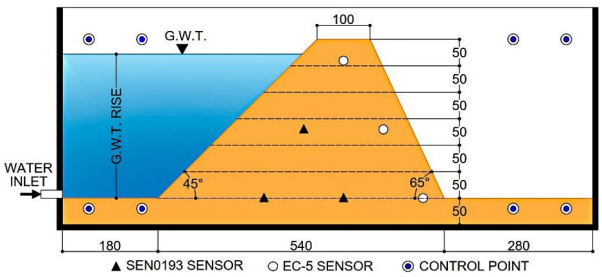

Fig. 3. Schematic illustration of the model.

Cameras and lighting setup:

During the experiment a visual range video was recorded with 1280x1024 pixel resolution at 30 fps using a Canon EOS 600D camera. A Scintacor CamIR infrared camera was used at video mode (640x480 pixels at 30 fps) to capture the infrared images, the used camera has a Sony ICX445 1/3" image sensor, after a phosphor treatment, the sensor showed two spectral sensitivity peaks at 1512 and 1540 nm. For image analysis, visual and infrared frames were extracted from

the videos taken with the previously mentioned cameras. The illumination setup was composed of five 175 W infrared light bulbs that were manually oriented to provide evenly distributed light intensity over the model surface.

Soil sample preparation:

The soil used in the experiment is a fine beach sandy soil from Castelldefels, Catalonia, Spain. Material properties are presented in Table 1. This material was previously calibrated [17] to get the Sr vs GVn correlation curve (Figure 2). The material was prepared with a gravimetric water content of 5% and was deposited in seven tamped layers of 50 mm. During model construction the mass deposited in each layer was quantified, an average density of 1.42 g/cm^3 was obtained.

Table 1. Castelldefels beach sand properties [17].

Parameter	Unit	Value
Particle density	g/cm^3	2.665
Dry density	g/cm^3	1.442 – 1.795
Porosity	-	0.459 – 0.326
Particle-size distribution		
D10	mm	0.254
D30	mm	0.3109
D60	mm	0.3715
Air-entry value	kPa	0.7
van Genuchten model parameters [18]		
$S_e = \frac{S_l - S_{rl}}{S_{ls} - S_{rl}} = \left[1 + \left(\frac{P_g - P_l}{P}\right)^{\frac{1}{1-\lambda}}\right]^{-\lambda}$; $P = P_0 \frac{\sigma}{\sigma_0}$		
Pore-water pressure at 20 ºC, P_0	MPa	0.0012
Surface tension at 20 ºC, σ_0	MPa	0.072
Shape parameter, λ	-	0.8
Minimum saturation, S_{rl}	-	0
Maximum saturation, S_{ls}	-	1.0

Note: S_e is the effective saturation, S_l is the relative saturation, $(P_g - P_l)$ suction equal to the difference between gas (P_g) and liquid (P_l) pressure.

Image analysis:

The PIV-NP [6] technique is selected to measure cumulative displacements, soil particle trajectories, velocities, and deformations occurred during the wetting process of the dam by imposing the water rise in one side. To measure the degree of saturation, infrared images were used along the SWIR-Sr technique [17] considering that soil surface reflectance is more sensitive to moisture variations on the SWIR range [11-17]. The consecutive frames for PIV-NP and SWIR-Sr were extracted from the recorded videos taken with the visual and infrared camera, respectively.

The total experiment duration of 810 seconds was divided into two stages to be analysed. The first stage corresponds to the water table rise (0 – 700 seg), while the second stage includes the triggering of the failure and the subsequent run-out (700 – 810 seg). A frame speed of 1 fps was selected for the first stage considering the small strains occurred until the trigger of the failure. For the second stage a frame speed of 30 fps was used to track the fast motion generated during failure.

4 Results

4.1 Motion description

The images captured at visual range allow a qualitative description of the motion observed during the experiment. It can be determined that the failure was triggered when the water table reached a height of 205 mm measured from the base of the dam, at this instant two features can be pointed out. First, the crown of the dam settled 9.7 mm during wetting. In second place, deformations at the toe of the dam started to increase. This was used as an indicator of the triggering of the failure. A few seconds later, specifically at 723 seconds of the experiment, a fast failure occurred. During the failure, two cracks suddenly appeared, crack #1 at 723 seconds and the crack #2 at 768 seconds (Figure 4). The location of both cracks coincides with the position of the E2 and E1 moisture sensors respectively. The cracks marked a significant boundary between two soil masses that moved independently. At the end of the test, a horizontal displacement of 87 mm at the toe of the downstream slope was manually measured.

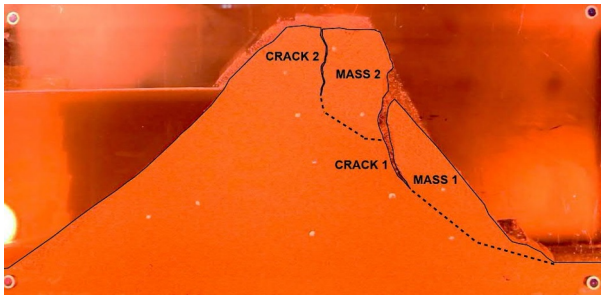

Fig. 4. Visual frame presenting the failure mechanism of the model.

4.2 Velocity and deformations: PIV-NP results

Consecutive frames were used for image analysis with the PIV-NP technique. The PIV-NP results allow evaluate the failure mechanism quantitatively and further interpretation of the test results. Figure 5(a) shows the NP velocities at 723.167 seconds of the test. At this time a velocity of 45.3 mm/s was measured, which was the maximum velocity detected during the test. The updated position of NPs and the velocity magnitude provide the visualization the failure mechanism described in Section 4.1. Figure 5(b) shows the results at the end of the experiment. A clear definition of both unstable soil masses can be appreciated with the updated position of the numerical particles. At the end of the experiment, a maximum accumulated displacement of 88.5 mm was measured in numerical particles of the first unstable soil mass. Some numerical particles that seem to float in the air can be observed in Figure 5(b). They correspond to sand particles that sticked to the transparent wall during the experiment.

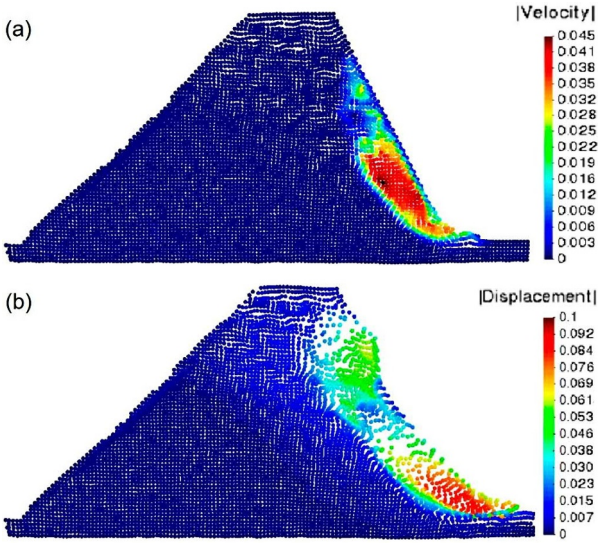

Fig. 5. PIV-NP results: (a) 2D velocity map at 723.167 seconds, and (b) 2D accumulated displacement map at the end of the test.

In addition, PIV-NP technique provides the motion of NPs. Figure 6 presents the accumulated displacement of two NP located in the mobilized mass. The two steps of failure are clearly observed with the sudden increment of displacement.

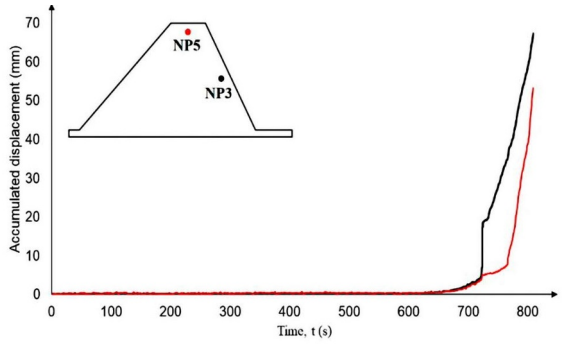

Fig. 6. PIV-NP accumulated displacement for two numerical particles.

4.3 Degree of saturation: SWIR-Sr results

High spatio-temporal resolution results of degree of saturation were calculated with the SWIR-Sr technique. Figure 7 presents 2D maps, correspond to the measurement of surface degree of saturation at 180 and 540 seconds. The values of degree of saturation mapped were calculated by correlating the normalised gray value (GVn) with the calibration curve (Sr vs GVn) of Castelldefels beach sand previously described by Parera *et al.* [17]. The water level was manually drawn over the SWIR-Sr results according to the water table level observed at the SWIR image frames. SWIR-Sr graphical results make possible a qualitative and quantitative interpretation of hydraulic behaviour such as the advance of the saturation front and the capillary zone. This represents a useful tool to analyse seepage flow in unsaturated porous media and coupled hydro-mechanical behaviour such as the loss of shear strength due to suction loss during wetting.

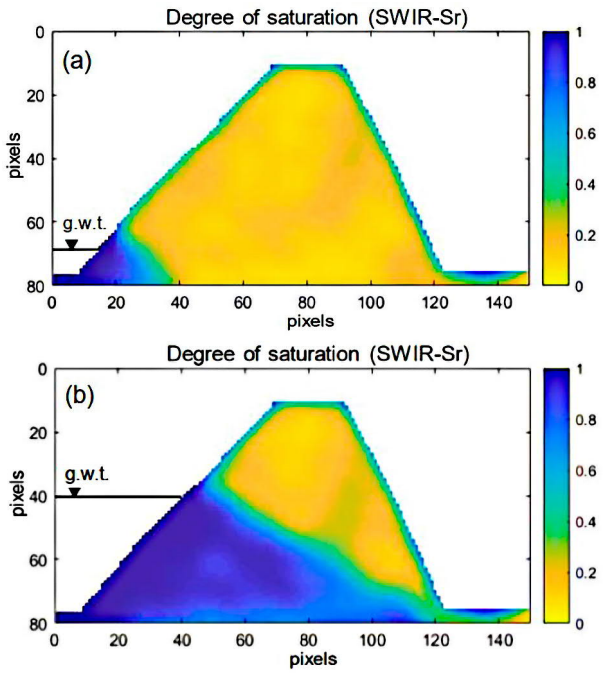

Fig. 7. SWIR-Sr results: (a) 2D map of surface degree of saturation at t = 180s; (b) 2D map of surface degree of saturation at t = 540s.

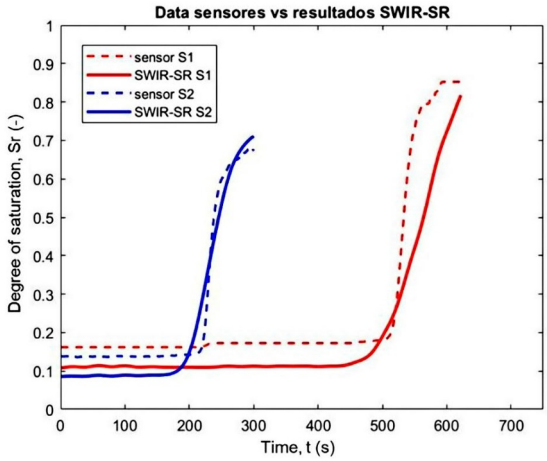

Fig. 8. Comparison between SWIR-Sr measurements of degree of saturation and capacitance moisture sensors readings

Soil moisture capacitance sensors were installed within the model to validate the SWIR-Sr results. During the wetting, the saturation front only reached the position of sensors S1, S2, S3 and E3. Sensor readings and SWIR-Sr results were compared since the wetting started until the arrival of the saturation front to the location of each sensor (see sensor locations in Figure 3). A comparison between SWIR-Sr results and the S1 and S2 sensor measurements is presented on Figure 8, good agreement between sensor measurements and SWIR-Sr results was achieved.

5 Conclusions and discussion

This paper presents the use of digital image as a non-invasive tool to evaluate a small-scale physical model of a dam made of fine beach sand. To measure cumulative displacement and velocities generated during the test,

visual range images were taken and the PIV-NP technique was applied. On the other hand, to measure the variations of the degree of saturation, infrared images and the SWIR-Sr technique were used. The experimental setup (transparent tank, lighting system, cameras and sensors), soil sample preparation, and image analysis approach, was presented and described.

Important features of the dynamic behaviour of the physical model during the test can be measured through the PIV-NP technique [6]. This image-based analysis technique allows the calculation of cumulative displacement, trajectories, velocities and deformations that are mapped to numerical particles which represent real soil portions. In the paper, the cumulative displacement and velocity variations in time are presented for two numerical particles (NP). The results show that the numerical particle NP3 suddenly accelerated at 723.2 seconds and reached a maximum speed of 38.6 mm/s.

The SWIR-Sr technique [17] was used to measure the variation of the degree of saturation at high spatio-temporal resolution through infrared images taken during the test. Validation of SWIR-Sr results was carried out by comparing the measurements of soil moisture sensors installed in the model. Moisture sensors measurements and SWIR-Sr results showed good agreement.

The use of digital images to analyse physical models has spread over the last decade among the geotechnical research community. The use of digital image correlation techniques represents an advantage over the use of traditional sensors because of its non-invasive nature and its high spatio-temporal data resolution. However, multiple factors could affect its performance; for example, PIV-NP calculations errors are observed specially in the contours. In addition, SWIR-Sr is highly dependent on the surface soil reflectance, which is represented as pixel intensity in infrared images. Reflectance can be altered during physical modelling by multiple factors such as: non-uniformity of incident light intensity over the whole experiment surface; electrical tension fluctuations during the experiment; and reflections generated by external objects located near the region of interest. Measurement of water content and degree of saturation on soil surface works on the principle that soil becomes darker when wetted, it is less reflective; for this reason, when using image analysis to measure the degree of saturation, reflectance must depend only on moisture variations over the soil surface.

Acknowledgments

The second author, as Associate professor Serra Húnter, gratefully acknowledges funding from the Departament de Recerca i Universitats de la Generalitat de Catalunya. This publication is part of the R&D&I project RTI2018-097365-B- funded by MCIN/ AEI/10.13039/ 501100011033, "ERDF A way of doing Europe". The authors gratefully acknowledge the financial support to CIMNE provided by CERCA/Generalitat de Catalunya program.

References

1. G. Morales, N.M. Pinyol, A. Lloret, X Simp. Nac. Taludes y Laderas Inest., **10**: 780-791 (2022)
2. R.J. Adrian, Annu. Rev. Fluid Mech., **23**: 261-304 (1991)
3. W. Thielicke, E.J. Stamhuis, J. Open Research Software, **2**: 2-10 (2014)
4. D.J. White, W.A. Take, M.D. Bolton, Géotechnique, **53**, No. 7: 619-631 (2003)
5. S.A. Stanier, J. Blaber, W.A. Take, D.J. White, Can. Geotech. J., **53**: 727-739 (2015)
6. N.M. Pinyol, M. Alvarado, Can. Geotech. J., **54**: 933-944, (2017)
7. S.A. Stanier, J. Dijkstra, D. Leśniewska, J. Hambleton, D.J. White, Comp. and Geotech., **72**: 100-113 (2016)
8. M. Persson, Vadose Zone J., **4**: 1119-1122 (2005)
9. N. Yoshimoto, R.P. Orense, F. Tanabe, N. Kikkawa, M. Hyodo, Y. Nakata, Soils and Found., **51**, No. 1: 167-177 (2011)
10. B. Belfort, S. Weill, F. Lehman, J. of Hydrology, **550**, 343-354 (2017)
11. S. Bowers, R. Hanks, Soil Sci., **100**: 130-138 (1965)
12. D. Lobell, G. Asner, Soil Sci. Soc. of Am. J., **66**, No. 3: 722-727 (2002)
13. M. Knadel, F. Deng, A. Alinejadian, J. Wollesen de Jonge, P. Moldrup, Soil Sci. Soc. of Am. J., **78**, No. 2: 422-433 (2014)
14. C. Nolet, A. Poortinga, P. Roosjen, H. Bartholomeus, G. Ruessink, PLoS ONE, **9**, No. 11: e112151 (2014)
15. M. Sadeghi, S.B. Jones, W.D. Philpot, Rem. Sen. of Environm., **164**: 66-76 (2015)
16. J. Tian, W.D. Philpot, Rem. Sen. of Environm., **169**: 280-289 (2015)
17. F. Parera, N.M. Pinyol, E.E. Alonso, Can. Geotech. J., **58**, 749-762 (2021)
18. M.T. van Genuchten, Soil Sci. Soc. of Am. J., **44**, No. 5: 892-898 (1980)